Journal of Magnetic Resonance **142,** 64–73 (2000)
Article ID jmre.1999.1903, available online at http://www.idealibrary.com on IDEAL®

Theoretical Study of Two-Dimensional COSY Experiments for $S = 7/2$ Spins: Application to ^{59}Co in the Tetrahedral Cluster $HFeCo_3(CO)_{11}PPh_2H$

Pierre Kempgens,* Jésus Raya,* Karim Elbayed,* Pierre Granger,* Jacky Rosé,† and Pierre Braunstein†

**UMR 50 CNRS-Bruker-Université Louis Pasteur, Institut de Chimie, BP 296, 67008 Strasbourg Cédex, France; and †Laboratoire de Chimie de Coordination, URA 416 CNRS, Université Louis Pasteur, 4 rue Blaise Pascal, 67070 Strasbourg Cédex, France*

Received January 20, 1999; revised August 10, 1999

The first investigation and analysis of ^{59}Co 2D NMR homonuclear chemical shift correlation spectra are reported for the tetrahedral mixed-metal cluster $HFeCo_3(CO)_{11}PPh_2H$. For this cluster in solution, the ^{59}Co 2D COSY and DQF COSY NMR spectra prove the existence of a scalar coupling between ^{59}Co nuclei. In order to obtain a value of this coupling, the 2D COSY and DQF COSY NMR spectra for a three-spin 7/2 AX_2 system have been simulated by numerical density matrix calculations. The comparison between experimental and theoretical 2D NMR spectra gives a spin-coupling constant $|^1J(^{59}Co - {}^{59}Co)| = (115 \pm 20)$ Hz for this cluster. Experimental measurements of T_1 and of the line widths for cobalt 59 as well as theoretical ^{59}Co 1D NMR spectra are reported and support our findings.

Key Words: **Cobalt-59 NMR; 2D COSY and DQF COSY NMR; scalar coupling; quadrupolar nuclei.**

I. INTRODUCTION

Two-dimensional (2D) NMR spectroscopy has proved to be a very powerful tool for studying dynamic process, determining coupling patterns, or separating different interactions (*1*). Among the various 2D NMR experiments for structural research, chemical shift correlations are without doubt the most useful. The first 2D experiment proposed by Jeener in 1971 (*2*) was a homonuclear chemical shift correlation or COSY experiment. The resulting 2D spectrum exhibits diagonal peaks corresponding to chemically different sites and cross-peaks if scalar spin–spin couplings exist between each sites. A particular attractive feature of the COSY experiment is that scalar couplings can be detected even when they are not resolved in the one-dimensional (1D) spectrum (*3–5*). However, very short relaxation times and/or very small scalar coupling may average the spin coupling interaction to zero and prevent the detection of cross-peaks. Therefore, COSY experiments are expected to be not instructive in the case of fast relaxing nuclei. Nevertheless, COSY experiments for quadrupolar nuclei have been so far successfully performed for ^{11}B (*3, 4, 6–12*), ^{51}V (*5*), ^{2}H (*13, 14*), ^{6}Li (*15–17*), and ^{7}Li (*16–18*). However, all of them imply very small quadrupolar moments and consequently relatively narrow lines ranging between 10 and 150 Hz.

Owing to the large quadrupole moment of 0.42×10^{-28} m^2, ^{59}Co in an unsymmetrical environment, as found in clusters, leads to broad lines that are often unobservable. Pioneering work (*19–21*) and more recent studies (*22–25*) have shown that ^{59}Co NMR measurements in heterometallic tetrahedral clusters lead to line widths of a few kHz which allow an easy observation of ^{59}Co NMR resonances. In the present paper, we want to report the first homonuclear ^{59}Co chemical shift correlation experiments and theoretical simulations which have been performed on the tetrahedral mixed-metal cluster $HFeCo_3(CO)_{11}PPh_2H$ (Fig. 1), even though the line widths of the peaks in the 1D ^{59}Co spectrum are greater than 1 kHz. Furthermore, the wide spectral width involved in ^{59}Co NMR led us to tackle these experiments using solid state NMR transmitters and probes to obtain very short pulses.

The related cluster provides an interesting system to observe for the first time a scalar coupling between cobalt nuclei using 2D COSY experiments and eventually to determine its magnitude. In order to provide confirmation of our results, a theoretically investigation based on density matrix calculations was performed. This investigation was done for 2D COSY and Double Quantum Filtered (DQF) COSY experiments in the case of a weakly coupled three-spin 7/2 system. The theoretically predictions will be used to investigate quantitatively the experimental 2D spectra in order to obtain a value for the scalar coupling between cobalt nuclei. It should be noted that until present, only one experimental and theoretical investigation of 2D COSY experiments involving quadrupolar nuclei has appeared in the literature (*17*). A numerical approach was used by Moskau *et al.* (*17*) to stimulate 2D COSY spectra for two-spin-1 and two-spin-3/2 systems. The determination of a scalar coupling between two quadrupolar nuclei provides very useful structural informations and opens up the opportunity of using this coupling to probe the bonding between transition metals in cluster compounds of the type studied here.

In the following, we shall briefly outline the theory of homonuclear 2D chemical shift correlation spectroscopy and discuss the 2D COSY and DQF COSY spectra of a three-spin-7/2 AX_2 system.

1090-7807/00 $35.00

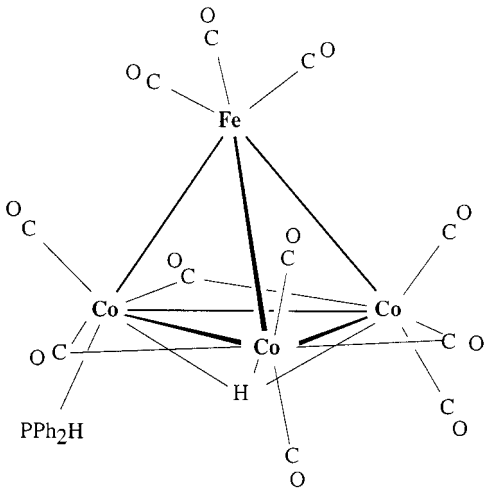

FIG. 1. Schematic of the $HFeCo_3(CO)_{11}PPh_2H$ cluster.

II. THEORY

The simplest COSY experiment is based on the sequence $(\pi/2)$–t_1–$(\pi/2)$–t_2. The first $(\pi/2)$ pulse applied to a spin system in thermal equilibrium, creates coherences $|t\rangle\langle u|$ for all allowed transitions between states $|t\rangle$ and $|u\rangle$. All coherences precess during the evolution time t_1 with their characteristic angular frequency $\omega_{u,t}$ around the z axis and decay with their transverse relaxation time $T_{2(t,u)}$. At the end of the evolution period a second $(\pi/2)$ pulse is applied. This mixing pulse partially transforms the coherence between two states $|t\rangle$ and $|u\rangle$ into coherence between two other states $|r\rangle$ and $|s\rangle$. At the end of this pulse all coherences $|r\rangle\langle s|$ evolve during the detection time t_2 with their characteristic angular frequency $\omega_{s,r}$ around the z axis and decay with their transverse relaxation time $T_{2(r,s)}$. During the detection time t_2, the transverse magnetization is acquired.

The time-independent Hamiltonian H which describes the Zeeman and chemical shift interactions of the nuclear spins with the external magnetic field as well as the scalar coupling of the spins among themselves is given by

$$H = \sum_{i=1}^{K} \Omega_i S_{zi} + \sum_{j<i}^{K} J_{ij}\mathbf{S}_i \cdot \mathbf{S}_j. \qquad [1]$$

In Eq. [1], the symbols have their usual meanings and the summations over i and j are over all the K nuclei of spin S in the spin system. In this work, the angular frequency variables

$$\omega_{\alpha,\beta} = \langle\alpha|H|\alpha\rangle - \langle\beta|H|\beta\rangle \qquad [2]$$

correspond to the offsets with respect to the carrier frequency.

The complex signal obtained by simultaneous observation of both x and y components by quadrature detection may be written as (*26*)

$$s^+(t_1, t_2) = i \sum_{r,s}^{N} \sum_{\substack{t,u \\ t>u}}^{N} Z_{r,s,t,u} \exp(-i\omega_{u,t}t_1)\exp(i\omega_{s,r}t_2) \times \exp(-t_1/T_{2(t,u)})\exp(-t_2/T_{2(r,s)}) \qquad [3]$$

with the complex factor (*1*)

$$Z_{r,s,t,u} = S^+_{s,r}\Re_{r,s,t,u}\sigma_{t,u}(t_1 = 0). \qquad [4]$$

In Eq. [3], N is the number of quantum states of the spin system. The complex intensity $Z_{r,s,t,u}$ defined in Eq. [4] contains three factors. The density matrix element $\sigma_{t,u}(t_1 = 0)$ represents the initial amplitude and phase of a coherence component associated with a transition $|t\rangle \leftrightarrow |u\rangle$ at the beginning of the evolution period. The selection rules of observation are represented by the raising operator matrix element $S^+_{s,r} = S_{x(s,r)} + iS_{y(s,r)}$, where S_x and S_y are the x and y components of the total angular momentum spin operator. The coherence transfer amplitude $\Re_{r,s,t,u}$ which describes the transfer of coherence from a transition between two states $|t\rangle$ and $|u\rangle$ to a transition between two other states $|r\rangle$ and $|s\rangle$ is equal to the product of two rotation matrix elements (*1*, *26*)

$$\Re_{r,s,t,u} = R^{-1}_{r,t}R_{u,s} = R^*_{t,r}R_{u,s}, \qquad [5]$$

where R is explicitly given by

$$R = \exp\left[-i\,\frac{\pi}{2}\,S_x\right]. \qquad [6]$$

The peak intensities are determined by the amplitudes of coherence transfer, taking into account the limitations imposed by coherence transfer selection rules. Equation [3] represents a signal modulated in phase as a function of t_1 from which the sign of the modulation frequency $\omega_{u,t}$ is automatically determined in a two-dimensional complex Fourier transformation (*27*).

Similar chemical shifts correlation information may be gained through the application of a multiple quantum correlation experiment (*28*). Double quantum filtration is probably the most widely applicable since it employs routine $(\pi/2)$ phase shifts. The modification to provide double quantum filtering of a COSY spectrum is quite simple since the normal COSY pulse sequence is followed by a third $(\pi/2)$ pulse whose phase is cycled independently of those of the two first $(\pi/2)$ pulses. Double quantum coherences are generated by the two first $(\pi/2)$ pulses and are converted into observable single quantum coherences by the additional pulse, while the filtering of single and higher order multiple quantum coherences is provided by the phase cycling. Since the evolution of double quantum coherences after the second $(\pi/2)$ pulse is not desired, the delay between the second and third $(\pi/2)$ pulses must be kept as short as technically possible (*29*). Indeed, the simplest DQF COSY

TABLE 1
The 8×8 Matrices S_z, S^+, and R for a Single Spin 7/2

$$S_z = \frac{1}{2}\begin{pmatrix} 7 & 0 & 0 & 0 & 0 & 0 & 0 & 0 \\ 0 & 5 & 0 & 0 & 0 & 0 & 0 & 0 \\ 0 & 0 & 3 & 0 & 0 & 0 & 0 & 0 \\ 0 & 0 & 0 & 1 & 0 & 0 & 0 & 0 \\ 0 & 0 & 0 & 0 & -1 & 0 & 0 & 0 \\ 0 & 0 & 0 & 0 & 0 & -3 & 0 & 0 \\ 0 & 0 & 0 & 0 & 0 & 0 & -5 & 0 \\ 0 & 0 & 0 & 0 & 0 & 0 & 0 & -7 \end{pmatrix}$$

$$S^+ = \begin{pmatrix} 0 & \sqrt{7} & 0 & 0 & 0 & 0 & 0 & 0 \\ 0 & 0 & 2\sqrt{3} & 0 & 0 & 0 & 0 & 0 \\ 0 & 0 & 0 & \sqrt{15} & 0 & 0 & 0 & 0 \\ 0 & 0 & 0 & 0 & 4 & 0 & 0 & 0 \\ 0 & 0 & 0 & 0 & 0 & \sqrt{15} & 0 & 0 \\ 0 & 0 & 0 & 0 & 0 & 0 & 2\sqrt{3} & 0 \\ 0 & 0 & 0 & 0 & 0 & 0 & 0 & \sqrt{7} \\ 0 & 0 & 0 & 0 & 0 & 0 & 0 & 0 \end{pmatrix}$$

$$R = \frac{1}{16}\begin{pmatrix} \sqrt{2} & i\sqrt{14} & -\sqrt{42} & -i\sqrt{70} & \sqrt{70} & i\sqrt{42} & -\sqrt{14} & -i\sqrt{2} \\ i\sqrt{14} & -5\sqrt{2} & -3i\sqrt{6} & \sqrt{10} & -i\sqrt{10} & 3\sqrt{6} & 5i\sqrt{2} & -\sqrt{14} \\ -\sqrt{42} & -3i\sqrt{6} & \sqrt{2} & -i\sqrt{30} & \sqrt{30} & -i\sqrt{2} & 3\sqrt{6} & i\sqrt{42} \\ -i\sqrt{70} & \sqrt{10} & -i\sqrt{30} & 3\sqrt{2} & -3i\sqrt{2} & \sqrt{30} & -i\sqrt{10} & \sqrt{70} \\ \sqrt{70} & -i\sqrt{10} & \sqrt{30} & -3i\sqrt{2} & 3\sqrt{2} & -i\sqrt{30} & \sqrt{10} & -i\sqrt{70} \\ i\sqrt{42} & 3\sqrt{6} & -i\sqrt{2} & \sqrt{30} & -i\sqrt{30} & \sqrt{2} & -3i\sqrt{6} & -\sqrt{42} \\ -\sqrt{14} & 5i\sqrt{2} & 3\sqrt{6} & -i\sqrt{10} & \sqrt{10} & -3i\sqrt{6} & -5\sqrt{2} & i\sqrt{14} \\ -i\sqrt{2} & -\sqrt{14} & i\sqrt{42} & \sqrt{70} & -i\sqrt{70} & -\sqrt{42} & i\sqrt{14} & \sqrt{2} \end{pmatrix}$$

experiment is based on the sequence $(\pi/2)$–t_1–$(\pi/2)$–$(\pi/2)$–t_2. The complex signal is obtained by simultaneous observation of both x and y components by quadrature detection. The required complex signal was calculated in a manner analogous to that described for the standard COSY experiment by adding the third $(\pi/2)$ pulse and taking into account the phase cycle (*26, 30*). A DQF COSY sequence allows the detection of signals from all coupled spin systems but suppresses single quantum coherence from singlets. The main advantage is that the DQF experiment generally reduces diagonal peak intensity to the level of the cross peaks.

III. COMPUTER SIMULATIONS

In our case, it is less prone to errors to consider at first a three-spin-7/2 AMX system and Eq. [1] becomes

$$H = \Omega_A S_{zA} + \Omega_M S_{zM} + \Omega_X S_{zX} + J_{AM} S_{zA} S_{zM} + J_{AX} S_{zA} S_{zX} + J_{MX} S_{zM} S_{zX}, \qquad [7]$$

where the hypothesis of first order is used. The matrices for the angular momentum operators S_{zA}, S_{zM}, and S_{zX} are built up by means of direct products of the corresponding single spin 8×8 matrix S_z (Table 1) and the 8×8 unit matrix E (*31*). The $(2S + 1)^3 = 8^3$ quantum states for the three-spin-7/2 *AMX* system are defined from $N = 1$ to $N = 512$, in the same order as they appear by forming the direct product

$$|7/2,\ 7/2,\ 7/2;\ m_A,\ m_M,\ m_X\rangle = |7/2;\ m_A\rangle \otimes |7/2;\ m_M\rangle \otimes |7/2;\ m_X\rangle, \qquad [8]$$

where m_A, m_M, and m_X are the quantum states of the single spin A, M, and X, respectively. Note that the quantum states defined by Eq. [8] are the eigenstates of the operator $S_{zT} = S_{zA} + S_{zM} + S_{zX}$. The matrix representation of the time independent Hamiltonian H (Eq. [7]), expressed in the eigenstates of S_{zT}, is diagonal. Thus, the transition frequencies $\omega_{\alpha,\beta}$ of Eq. [2] are simply formed from the differences of components in H expressed in the eigenstates of S_{zT}. Even in the case of 512×512 matrices, it is relatively easy to derive analytical expressions of the transition frequencies. Therefore, the complex intensities $Z_{r,s,t,u}$ are the central quantities which have to be computed in Eq. [3]. The matrices for the raising and the rotation operators of the spin system are given by (*32*)

$$S_T^+ = S_A^+ + S_M^+ + S_X^+$$

$$R_T = R_A \cdot R_M \cdot R_X \qquad [9]$$

and are built up by means of direct products (*31*). The 8×8 matrices S^+ and R are defined in Table 1. At thermal equilibrium, the density matrix σ_{eq} is assumed to be equal to S_{zT} and the density matrix at the beginning of the evolution period is expressed as

$$\sigma(t_1 = 0) = R_T^{-1}\sigma_{eq}R_T = R_T^{-1}S_{zT}R_T. \quad [10]$$

For a three-spin-7/2 system, there are $(512)^4$ complex intensities $Z_{r,s,t,u}$ and these factors were calculated numerically with a program written in FORTRAN 77. The knowledge of the complex intensities allows us to expand Eq. [3] and a second program written in C uses the expressions we have obtained to compute the free induction decays for incremented values of t_1. In both cases, calculations were performed on a Silicon Graphics Computer (MIPS R4000 SC monoprocessor) with programs written by the authors. The complex arithmetic was implemented with double precision floating point numbers. The generation of 128×512 data matrices containing the time domain signals for a three weakly coupled spin-7/2 system required 8 min.

In a second step, we will suppose that our three-spin-7/2 AX_2 system may be treated as a three-spin-7/2 *AMX* system, where $J_{AX} = J_{AM}$, $J_{MX} = 0$, and $\omega_M = \omega_X$. This approach is valid as long as multiexponential relaxation among the equivalent spins can be excluded (*1*). This is verified since, as will be seen later, the decay of coherences for nuclei *A* and *X* in the three-spin-7/2 AX_2 system is described by a single transverse relaxation times T_{2A} and T_{2X}, respectively. For an AX_2 weakly coupled spin system, the relation $|\omega_A - \omega_X| \gg |2\pi J_{AX}|$ still holds and the peak intensities depend on the two transverse relaxation times T_{2A} and T_{2X} and also on the value of J_{AX}. Figures 2 and 3 illustrate the effect of the transverse relaxation times T_{2A} on the intensities of the peaks, using, in the calculations of $s^+(t_1, t_2)$, a set of values corresponding to those found experimentally on our tetrahedral cluster. Figures 2a–2f (COSY) and 3a–3f (DQF COSY) are generated for $\omega_A = 4000$ Hz, $\omega_X = -3000$ Hz, $J_{AX} = 100$ Hz, $T_{2X} = 500$ μs, and $T_{2A} = 100$, 200, 300, 400, 500, and 1000 μs, respectively. Data were apodized in both dimensions by a squared sine bell function with $\pi/2$ shift. The data matrix $S(\omega_1, \omega_2)$ obtained after Fourier transformation of $s^+(t_1, t_2)$ in both domains is drawn in the power mode as a contour plot. As expected, these 2D spectra are symmetrical about the diagonal, i.e., $S(\omega_1, \omega_2) = S(\omega_2, \omega_1)$, and independent of the sign of the coupling constant J_{AX}.

These simulations show that if scalar coupling is present between two nuclei *A* and *X*, short transverse relaxation times of one of these two nuclei can attenuate the intensity of the cross peaks. Moreover, the vanishing of cross peaks may occur in situations with small coupling and very short relaxation times. Note particularly that even for a small coupling constant and relatively short relaxation times where the multiplet structure is not apparent in the 1D spectrum, it is nevertheless possible to detect small cross peaks in a 2D COSY spectrum. On the other hand, and for similar cases, these cross peaks appear to be comparable to the diagonal peaks in a 2D DQF COSY spectrum. The 2D COSY simulations in Fig. 2 also show the particular shape of cross peaks more marked for high T_{2A} values. From the simulations of 2D COSY spectrum (Fig. 2) and contrary to those of 2D DQF COSY spectrum (Fig. 3), it should finally be noted that the maximum of the cross peaks correspond to frequencies slightly different from (ω_A, ω_X) and (ω_X, ω_A). This feature comes from the fact we are facing some overlapping problems. As can be observed from Fig. 2, diagonal peaks are high enough to provide feet of comparable intensity relative to cross peaks. Keeping in mind these cross peaks have in-phase and anti-phase components, an enhancement of the formers is expected while the latters are partially or totally canceled with diagonal peaks feet. As a result, distorted cross peaks with positions shifted toward their in-phase components are observed. This effect is well exemplified in Fig. 2. In Fig. 2a, as there is not any cross peak, the diagonal peak exhibits a classical shape with its wings following a linear trajectory. In Figs. 2a to 2f increasing values of $|^1J(^{59}\text{Co}–^{59}\text{Co})|$ give stronger effects on the diagonal peaks wings. Those feet which are overlapping with cross peaks deviate more and more from the linear trajectory. They seem to "avoid" cross peaks and this arises from their cancellation with the latter cross peaks anti-phase components. On the other hand, 2D DQF COSY (Fig. 3) do not show this phenomenon. It can be seen that diagonal peaks feet are negligible relative to cross peaks, so there is not any overlapping effect. Undistorted diagonal and cross peaks are obtained and appear at the expected frequencies.

It is of interest to note that these deviations from right frequencies form a way to decide if a cross peak is a true one or a simple wing superimposition artifact. In this case, diagonal peak wing superimposition would lead to an additive scheme in such a way that no shape deviations would be observed. These artifacts would appear unshifted from exact frequencies. This will be illustrated in the last section.

IV. EXPERIMENTAL

The cluster $HFeCo_3(CO)_{11}PPh_2H$ has been synthesized from the tetranuclear mixed metal carbonyl hydride $HFeCo_3(CO)_{12}$ and PPh_2H according to the published procedure (*22*). Figure 1 presents the structure of this compound which was dissolved in $CDCl_3$. The concentration was around 0.02 M. ^{59}Co NMR measurements were carried out on a Bruker MSL 300 spectrometer operating at $B_0 = 7.1$ T. The corresponding ^{59}Co Larmor frequency is 71.213 MHz. Chemical shifts are reported downfield from the external reference $K_3Co(CN)_6$ saturated in D_2O. The temperature, $T \approx 300$ K for all the experiments, was regulated with a Bruker B-VT 1000 unit. Experiments were performed using a Bruker MAS probe with a cylindrical 7-mm zirconium rotor. This allows us to use a short $\pi/2$ pulse length of 2.25 μs necessary to cover adequately the whole spectrum.

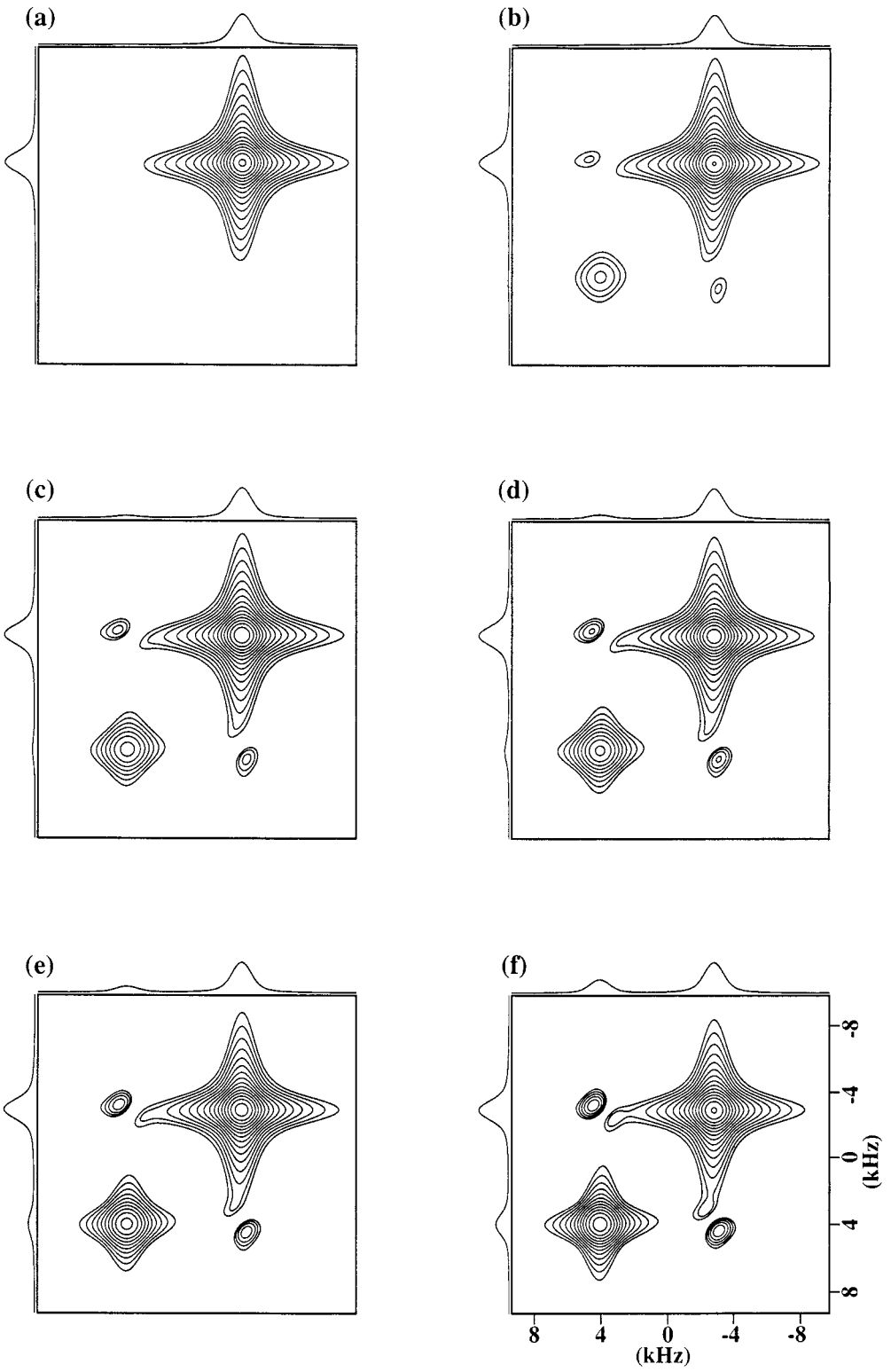

FIG. 2. Theoretical 2D NMR COSY power spectra for a three-spin-7/2 AX_2 system. Contour plots (a) to (f) correspond to $\omega_A = 4000$ Hz, $\omega_X = -3000$ Hz, $J_{AX} = 100$ Hz, $T_{2X} = 500$ μs, and $T_{2A} = 100$, 200, 300, 400, 500, and 1000 μs, respectively.

The ^{59}Co COSY spectrum of $HFeCo_3(CO)_{11}PPh_2H$ was obtained using the subprogram COSYN.PC from Bruker with the following parameters: SW1 = SW2 = 50 kHz, acquisition time 10.24 ms, 512 points, recycle delay 125 ms, 2720 scans, 128 decays in F1, squared sine bell apodization with $\pi/2$ shift and power spectra in both dimensions. The interpulse delay t_1

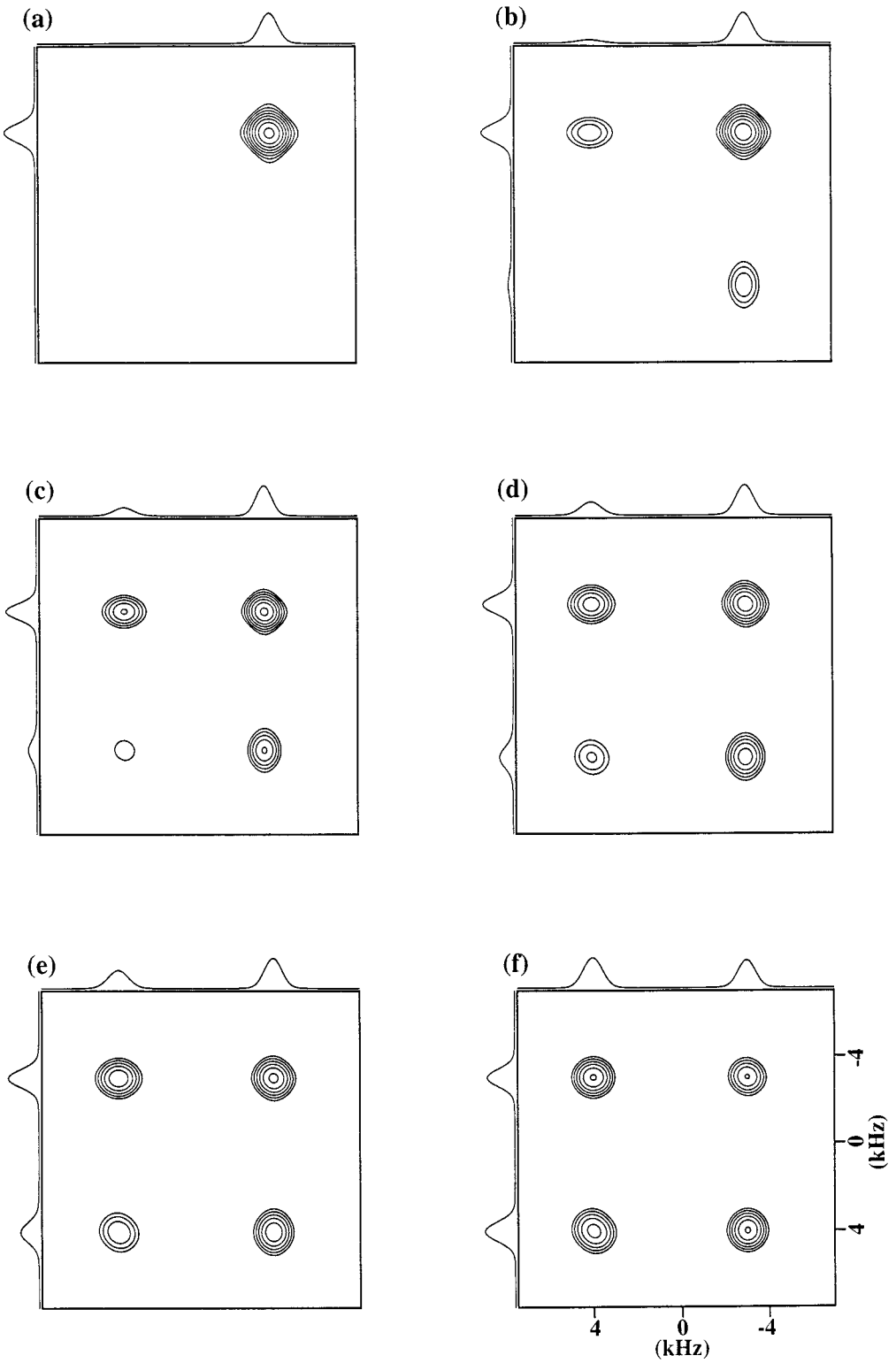

FIG. 3. Theoretical 2D NMR DQF COSY power spectra for a three-spin-7/2 AX_2 system. Contour plots (a) to (f) correspond to $\omega_A = 4000$ Hz, $\omega_X = -3000$ Hz, $J_{AX} = 100$ Hz, $T_{2X} = 500$ μs, and $T_{2A} = 100$, 200, 300, 400, 500, and 1000 μs, respectively.

was incremented by the dwell time and the transmitter frequency was placed within the middle of the spectrum. The ^{59}Co DQF COSY spectrum was obtained using the subprogram COSYDQ.PC from Bruker with the same parameters as for the ^{59}Co COSY spectrum, except for the number of scans which was equal to 3584.

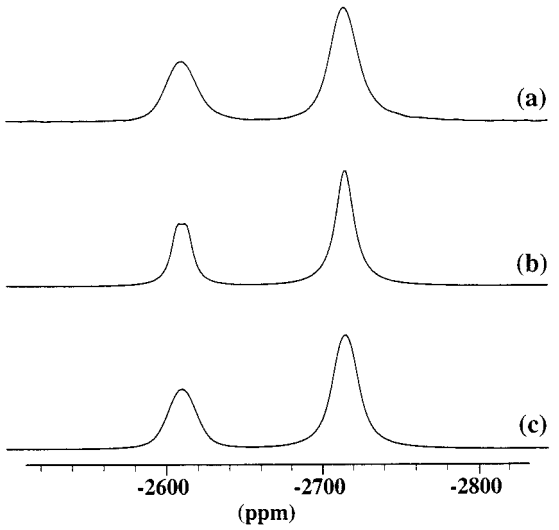

FIG. 4. ^{59}Co NMR spectra of the cluster $HFeCo_3(CO)_{11}PPh_2H$. (a) Experimental spectrum in $CDCl_3$ at $T = 300$ K. (b) Theoretical spectrum with $T_2(Co1) = 470$ μs, $T_2(Co2) = 330$ μs, and $^1J(^{59}Co1–^{31}P) = 450$ Hz. (c) Theoretical spectrum with $T_2(Co1) = 470$ μs, $T_2(Co2) = 330$ μs, $^1J(^{59}Co1–^{31}P) = 450$ Hz, and $^1J(^{59}Co1–^{59}Co2) = 120$ Hz.

For T_1 measurements of ^{59}Co nuclei, the standard inversion–recovery sequence, (π)–τ–$(\pi/2)$–Acquisition, was used. We have taken up to 350 scans and at least 22 values of τ for each T_1 measurement. The peak areas were used in a nonlinear three-parameter least-squares fit of data according to the usual equation: $I(\tau) = I_{eq}(1 - K \exp(-\tau/T_1))$. As the frequency difference between the two resonances is large, we verified that two measurements with the carrier frequency set at the resonance of each ^{59}Co nuclei and one measurement with the carrier frequency set within the middle of the spectrum give the same relaxation times. The maximum errors on T_1 values are estimated to be less than 10%. $T_2(^{59}Co)$ values were estimated from the line widths $\Delta\nu_{1/2}$.

V. RESULTS AND DISCUSSION

The ^{59}Co spectrum of the cluster $HFeCo_3(CO)_{11}PPh_2H$ presents two resonances having intensities in the ratio 2:1 (Fig. 4a). The cobalt nucleus bound to the phosphine ligand (Co1) is found at -2610 ppm while the two other equivalent nuclei (Co2) are observed at -2714 ppm. The direct measurement of the longitudinal relaxation times gives $T_1(Co1) = (470 \pm 40)$ μs and $T_1(Co2) = (320 \pm 30)$ μs. For both cobalt nuclei, the inversion–recovery sequence leads to a monoexponential behavior and excellent agreement between the experimental data points and the theoretical recovery curves is obtained. On the other hand, it has been recently shown (*33*) that the cobalt relaxation times T_1 for this cluster are temperature dependent but not field dependent. This result shows, in addition to the extreme narrowing conditions, that the ^{59}Co relaxation is dominated, as previously observed on analog compounds (*34*, *35*), by the quadrupolar relaxation mechanism, i.e., $T_1 = T_2$. Nevertheless, the T_2 values of Co1 and Co2 estimated from the line widths $\Delta\nu_{1/2}$ are around 190 μs far below the T_1 values. Moreover, the analysis of the ^{31}P saddle shaped spectra has given a value of $^1J(^{31}P–^{59}Co1) \approx 450$ Hz for this compound (*33*) and the line width of the peak corresponding to the two equivalent cobalt nuclei Co2 is expected to be essentially unaffected by the coupling constant between ^{59}Co and ^{31}P nuclei. The explanation of this difference between T_1 and T_2 is given by the existence of a scalar relaxation of the second kind, where T_1 is different from T_2. This mechanism implies a coupling constant which can be estimated with

$$\frac{1}{T_2(Co2)} - \frac{1}{T_1(Co2)} = \frac{4\pi^2}{3} J^2 S(S+1) T_2(Co1). \quad [11]$$

If we take the T_1 values previously obtained, $T_2(Co2) = 190$ μs and taking into account that a Co2 nucleus has a relaxation mechanism of the second kind arising from nucleus Co1, one obtains $^1J(^{59}Co1–^{59}Co2) = 165$ Hz. Furthermore, it was possible to compare the simulation of the ^{59}Co 1D spectrum obtained after Fourier transformation of the first free induction decay from the COSY experiment, corresponding to a short evolution time. The experimental line widths (Fig. 4a) are significantly larger than those obtained by considering the relaxation data, taking into account the scalar coupling of $^1J(^{31}P–^{59}Co1) = 450$ Hz for the cobalt nucleus bound to the phosphine ligand (Fig. 4b). These results provide further support for the presence of other unresolved coupling in the 1D spectrum. On the other hand, Fig. 4c shows that the simulation of the ^{59}Co 1D spectrum, taking into account the experimental chemical shifts and relaxation times $T_1(Co1)$ and $T_1(Co2)$ as well as the coupling constants $^1J(^{59}Co1–^{31}P) = 450$ Hz and $^1J(^{59}Co1–^{59}Co2) = 120$ Hz is in good agreement with the experimental ones of Fig. 4a. It was therefore of interest to obtain the ^{59}Co COSY spectrum of our cluster. In addition, the use of the double quantum correlation experiment could provide information frequently obscured in the 2D COSY experiment by the overlap of intense diagonal peaks with the cross peaks.

The 2D ^{59}Co COSY and DQF COSY NMR spectra are shown in Figs. 5a and 6a, respectively. In the 2D COSY NMR spectrum, cross peaks between the two resonances are weak but clearly resolved. One of the best proof that these cross peaks are not arising from overlapping of the long wings of the lines is provided by the DQF COSY NMR spectrum. In order to obtain a value of $|^1J(^{59}Co–^{59}Co)|$, the 2D ^{59}Co COSY and DQF COSY spectra were analyzed according to the formalism described above. In this analysis, it has been assumed that (a) the ^{59}Co relaxation is described with the assumptions of extreme narrowing and single correlation time and (b) the decay of coherences for nuclei A and X is described by a single transverse relaxation times T_{2A} and T_{2X}, respectively. To take into account the coupling between ^{59}Co and ^{31}P nuclei, the calculations were done by considering a free induction decay

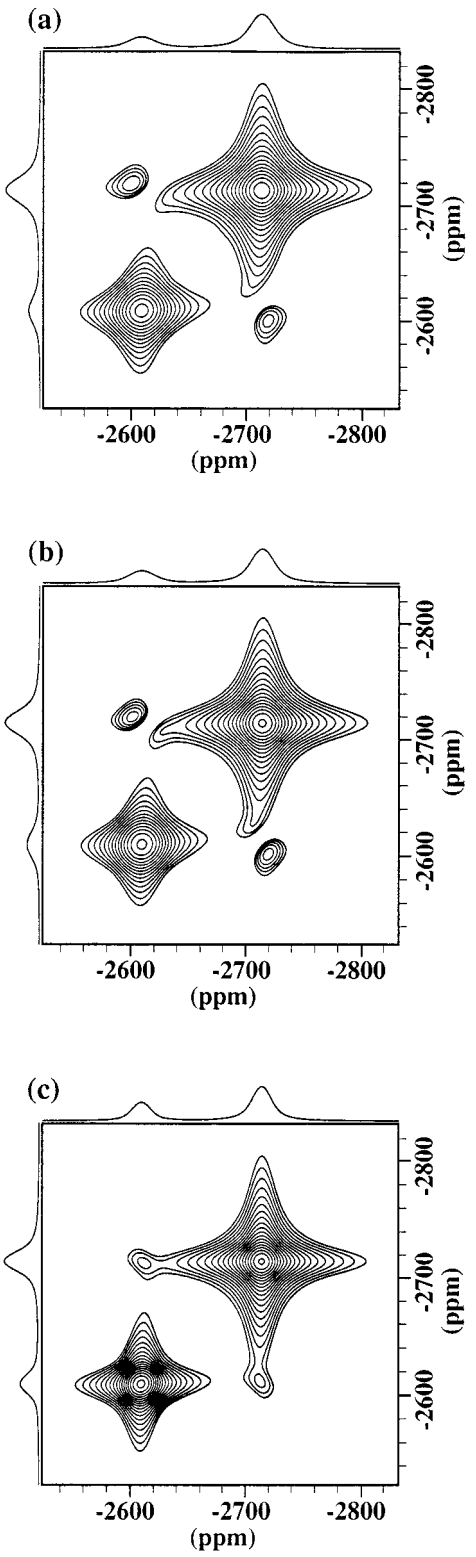

FIG. 5. ^{59}Co 2D NMR COSY power spectra of the cluster $HFeCo_3(CO)_{11}PPh_2H$. (a) Experimental spectrum in $CDCl_3$ at $T = 300$ K. (b) Theoretical spectrum with T_2(Co1) = 470 μs, T_2(Co2) = 330 μs, $^1J(^{59}\text{Co1}-^{31}\text{P})$ = 450 Hz and $^1J(^{59}\text{Co1}-^{59}\text{Co2})$ = 115 Hz. (c) Theoretical spectrum with T_2(Co1) = 470 μs, T_2(Co2) = 330 μs, $^1J(^{59}\text{Co1}-^{31}\text{P})$ = 450 Hz, and $^1J(^{59}\text{Co1}-^{59}\text{Co2})$ = 0 Hz.

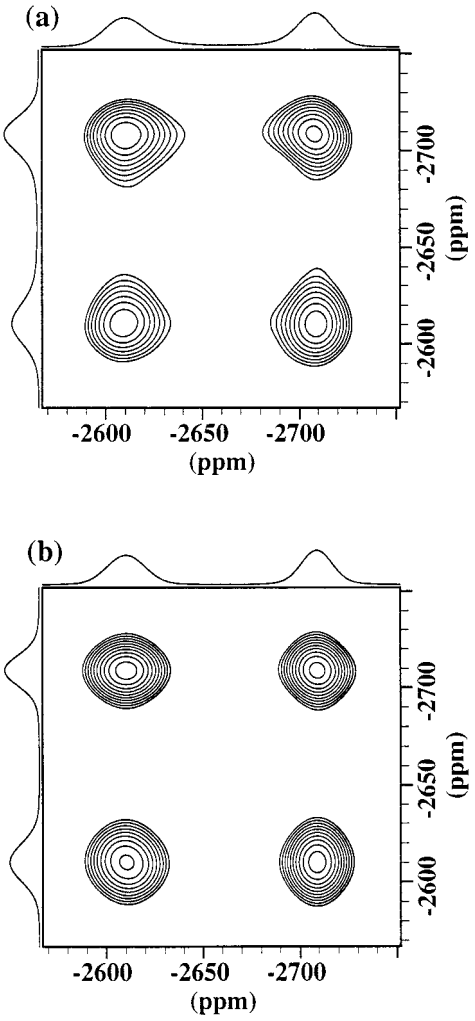

FIG. 6. ^{59}Co 2D NMR DQF COSY power spectra of the cluster $HFeCo_3(CO)_{11}PPh_2H$. (a) Experimental spectrum in $CDCl_3$ at $T = 300$ K. (b) Theoretical spectrum with T_2(Co1) = 470 μs, T_2(Co2) = 330 μs, $^1J(^{59}\text{Co1}-^{31}\text{P})$ = 450 Hz, and $^1J(^{59}\text{Co1}-^{59}\text{Co2})$ = 115 Hz.

as the sum of two ones calculated with a shift of the offset frequency corresponding to the cobalt nucleus bound to the phosphine ligand equal to $+\pi^1\text{J}(^{59}\text{Co1}-^{31}\text{P})$ and to $-\pi^1\text{J}(^{59}\text{Co1}-^{31}\text{P})$.

Experimental and simulated results for the related cluster are shown in Figs. 5a and 5b (COSY) and 6a and 6b (DQF COSY). The best parameters used to generate the calculated ^{59}Co COSY and DQF COSY spectra of Figs. 5b and 6b are T_2(Co1) = 470 μs, T_2(Co2) = 330 μs, $|J_{\text{Co1–Co2}}| = (115 \pm 20)$ Hz. The error is reported on the basis of the accuracy estimated for simulation observations. This error limit of $\pm 17\%$ is probably underestimated in view of unknown errors due to the assumptions used in the determination of $^1J(^{59}\text{Co}-^{59}\text{Co})$. Note that the relaxation times used for these simulations are in good agreement with those obtained by the inversion–recovery sequence. On the other hand, the experimental and simulated spectra are very similar. As can be seen in Figs. 5 and 6, the

experimental spectra mimic well the features of the predicted spectra in the presence of scalar coupling between cobalt nuclei. Finally and for comparison, Fig. 5c shows the ^{59}Co COSY spectrum generated with the same parameters as in Fig. 5b, except for the coupling constant $J_{\mathrm{Co1-Co2}}$, which was set equal to 0. As can be seen, the maximum height of the two cross peaks corresponds to the frequencies of the diagonal peaks. This is not the case in the presence of the scalar coupling where the maximum intensities are slightly shifted from the frequencies of the peaks positions. This feature, in addition to the shape of the peaks, can be used as an indication of the presence of a scalar coupling between quadrupolar nuclei.

It is of interest to compare this only known $^1J(^{59}\mathrm{Co}-^{59}\mathrm{Co})$ data to other metal to metal coupling available from the literature. For transition metal clusters, the actual measured values were recently reviewed (*36*). The relevant data corresponding to the situation of the related metal can be summarized as follow. Considering the reduced coupling constant $K = 4\pi^2 J/h\gamma^2$, for ^{195}Pt the corresponding ^1K values range between 180 and 1320 $\mathrm{NA}^{-2}\ \mathrm{m}^{-3}$ (*36*). For ^{109}Ag (*37*) and ^{103}Rh (*38*) the reported ^1J coupling constants give 160 and 84.5 $\mathrm{NA}^{-2}\ \mathrm{m}^{-3}$, respectively. The $^1J(^{59}\mathrm{Co}-^{59}\mathrm{Co})$ value obtained in this work leads to $^1K\ (^{59}\mathrm{Co}-^{59}\mathrm{Co}) = 17\ \mathrm{NA}^{-2}\ \mathrm{m}^{-3}$. Compared with ^{109}Ag and ^{103}Rh this result is satisfactory taking into account the fact that the chemical situation is different and that the contributions of *s* orbital to the coupling constant depends on the atom. Comparison with ^{195}Pt is not so easy since this atom is a heavy nucleus and relativistic effects lead to an increase of the coupling constant arising from the compression of the *s* orbitals.

VI. CONCLUSION

It was not obvious that the 2D COSY and DQF COSY experiments involving ^{59}Co would be instructive. Not only is $^{59}\mathrm{Co}-^{59}\mathrm{Co}$ coupling never resolved in the 1D spectrum but also relaxation times for ^{59}Co nuclei are usually very short, suggesting that relaxation would average the spin–spin coupling interaction to zero. However, we have shown that homonuclear ^{59}Co 2D NMR can successfully be applied to the study of tetrahedral clusters where a spin–spin coupling $^1J(^{59}\mathrm{Co}-^{59}\mathrm{Co})$ can occur. In order to obtain a value of the coupling constant between ^{59}Co nuclei, it was necessary to measure both the 2D COSY and DQF COSY NMR spectra and the longitudinal relaxation times. Due to the wide spectral widths involved in ^{59}Co NMR, very short radiofrequency pulses were needed and therefore implied the use of solid state NMR transmitters and probes. Nevertheless, a quantitative treatment of the ^{59}Co COSY and DQF COSY spectra based on the peak intensities has given for the first time the value of a coupling constant $^1J(^{59}\mathrm{Co}-^{59}\mathrm{Co})$. Note that these experiments are also possible for other similar clusters for which the 2D COSY and DQF COSY spectra are closely akin to those reported. Their analysis and studies will form the subject of future publications. Finally, it is also clear that similar results may be obtained on other transition-metal clusters containing quadrupolar nuclei with comparable or smaller quadrupole moment and high receptivity such as ^{45}Sc, ^{51}V, ^{55}Mn, and ^{95}Nb.

ACKNOWLEDGMENT

The UMR 50 CNRS–Bruker–ULP thanks the region Alsace for its participation in the purchase of the Bruker MSL 300 spectrometer.

REFERENCES

1. R. R. Ernst, G. Bodenhausen, and A. Wokaun, "Principles of Nuclear Magnetic Resonance in One and Two Dimensions," Clarendon, Oxford (1987).
2. J. Jeener, Ampere International Summer School, Basko Polje, Yugoslavia (1971).
3. D. Reed, *J. Chem. Res.* 198 (1984).
4. T. L. Venable, W. C. Hutton, and R. N. Grimes, *J. Am. Chem. Soc.* **106,** 29 (1984).
5. P. J. Domaille, *J. Am. Chem. Soc.* **106,** 7677 (1984).
6. T. L. Venable, W. C. Hutton, and R. N. Grimes, *J. Am. Chem. Soc.* **104,** 4716 (1982).
7. S. Hermanek, J. Fusek, B. Stibr, J. Plesek, and T. Jelinek, *Polyhedron* **5,** 1873 (1986).
8. G. B. Jacobsen, D. G. Meina, J. H. Morris, C. Thomson, S. J. Andrews, D. Reed, A. J. Welch, and D. F. Gaines, *J. Chem. Soc., Dalton Trans.* 1645 (1985).
9. X. L. R. Fontaine, H. Fowkes, N. N. Greenwood, J. D. Kennedy, and M. Thornton-Pett, *J. Chem. Soc., Dalton Trans.* 547 (1986).
10. X. L. R. Fontaine, H. Fowkes, N. N. Greenwood, J. D. Kennedy, and M. Thornton-Pett, *J. Chem. Soc., Dalton Trans.* 1431 (1987).
11. X. L. R. Fontaine, N. N. Greenwood, J. D. Kennedy, and P. MacKinnon, *J. Chem. Soc., Dalton Trans.* 1785 (1988).
12. B. H. Goodreau and J. T. Spencer, *Inorg. Chem.* **31,** 2612 (1992).
13. N. Chandrakumar and A. Ramamoorthy, *J. Am. Chem. Soc.* **114,** 1124 (1992).
14. D. Moskau and H. Günther, *Angew. Chem., Int. Ed. Engl.* **26,** 156 (1987).
15. H. Günther, D. Moskau, R. Dujardin, and A. Maercker, *Tetrahedron Lett.* **27,** 2251 (1986).
16. H. Günther, D. Moskau, P. Bast, and D. Schmalz, *Angew. Chem. Int. Ed. Engl.* **26,** 1212 (1987).
17. D. Moskau, W. Frankmölle, O. Eppers, H.-E. Mons, and H. Günther, *Proc. Indian Acad. Sci.* **106,** 1471 (1994).
18. D. Barr, W. Clegg, S. M. Hodgson, R. E. Mulvey, D. Reed, R. Snaith, and D. S. Wright, *J. Chem. Soc., Dalton Trans.* 367 (1988).
19. S. Aimé, R. Gobetto, D. Osella, L. Milone, G. E. Hawkes, and E. W. Randall, *J. Magn. Reson.* **65,** 308 (1985).
20. M. Hidai, H. Matsuzaka, Y. Koyazu, and Y. Uchida, *J. Chem. Soc., Chem. Commun.* 1451 (1986).
21. H. Matsuzaka, T. Kodama, Y. Uchida, and M. Hidai, *Organometallics* **7,** 1608 (1988).
22. P. Braunstein, J. Rosé, P. Granger, J. Raya, S. E. Bouaoud, and D. Grandjean, *Organometallics* **10,** 3686 (1991).
23. P. Braunstein, J. Rosé, P. Granger, and T. Richert, *Magn. Reson. Chem.* **S31,** (1991).
24. P. Braunstein, L. Mourey, J. Rosé, P. Granger, T. Richert, F. Balegroune, and D. Grandjean, *Organometallics* **11,** 2628 (1992).

25. T. Richert, K. Elbayed, J. Raya, P. Granger, P. Braunstein, and J. Rosé, *Magn. Reson. Chem.* **34,** 689 (1996).

26. A. Bax, "Two Dimensional Nuclear Magnetic Resonance in Liquids," D. U. Press, Dordrecht, Holland (1982).

27. A. Bax, R. Freeman, and G. A. Morris, *J. Magn. Reson.* **42,** 164 (1981).

28. U. Piantani, O. W. Sorensen, and R. R. Ernst, *J. Am. Chem. Soc.* **104,** 6800 (1982).

29. W. R. Croasmun and R. M. K. Carlson, "Two-Dimensional NMR Spectroscopy: Applications for Chemists and Biochemists" (A. P. Marchand, Ed.), VCH, Denton, Texas (1994).

30. G. E. Martin and A. S. Zektzer, "Two-Dimensional NMR Methods for Establishing Molecular Connectivity" (A. P. Marchand, Ed.), VCH, Denton, Texas (1988).

31. E. R. Johnston, *Concepts Magn. Reson.* **7,** 219 (1995).

32. T. C. Farrar, *Concepts Magn. Reson.* **2,** 55 (1990).

33. P. Granger, K. Elbayed, J. Raya, P. Kempgens, and J. Rosé, *J. Magn. Reson. A* **117,** 179 (1995).

34. P. Granger, T. Richert, K. Elbayed, P. Kempgens, J. Hirschinger, J. Raya, J. Rosé, and P. Braunstein, *Mol. Phys.* **92,** 895 (1997).

35. P. Kempgens, J. Hirschinger, K. Elbayed, J. Raya, P. Granger, and J. Rosé, *J. Phys. Chem.* **100,** 2045 (1996).

36. P. Granger, "Advanced Applications of NMR to Organometallic Chemistry" (M. Gielen, R. Willem, and B. W., Eds.), Wiley, Chichester, UK (1996).

37. S. S. D. Brown, I. J. Colquhoun, W. M. Farlane, M. Murray, I. D. Salter, and V. Sik, *J. Chem. Soc., Chem. Commun.* 53 (1986).

38. A. Nutton, P. M. Bailey, and P. M. Maitlis, *J. Organomet. Chem.* **213,** 313 (1981).